Data Repository Item DR2008225

Microorganisms

Virgibacillus marismortui AJ009793 is a gram-positive, endospore-forming, rod shaped, chemoorganotrophic and strictly aerobic bacterium. The growth temperature ranges from 15 to 50˚C (optimal at 37˚C) (Arahal et al., 1999). This strain was isolated from Brejo do Espinho (Rio de Janeiro, Brazil), a shallow hypersaline coastal lagoon in which dolomite precipitates (Sánchez-Román, 2006; Sánchez-Román et al., in press). It was first isolated from the Dead Sea and was originally described as *Bacillus marismortui* (Arahal et al., 1999).

Halomonas meridiana ACAM 246 (= UQM 3352) is a gram-negative, nonspore-forming, rod shaped, chemoorganotrophic and strictly aerobic bacterium. Its maximum growth temperature is 45˚C (James et al., 1990). *H. meridiana* was isolated in 1990 from Antarctic saline lakes (James et al., 1990).

Both *V. marismortui* and *H. meridiana* are moderately halophilic aerobic bacteria. They are highly useful to determine how the ionic composition of the environment affects the bacterial precipitation of minerals because they both grow under widely varying saline concentrations. Such halophilic microorganisms are abundant in hypersaline lakes and in other habitats characterized by salt concentrations approaching halite saturation, and they have a strong impact on the ecosystems in which they thrive (Oren, 2002).

Culture medium

The experiments were conducted using the D-1 medium (Sánchez-Román, 2006; Sánchez-Román et al., *in press*) designed with the following composition, (%, wt/vol): 1 % yeast extract; 0.5% proteose peptone; 0.1% glucose, 3.5% NaCl and supplemented with 84 mM Mg^{2+}; 11 mM Ca^{2+}. To obtain a solid medium, 20 g/l Bacto-Agar was added. The pH was adjusted to 7.2 with 0.1 M KOH and the solution was sterilized at 121˚C for 20 minutes.

Recovering of minerals from plates

The Petri dishes were sealed with parafilm to avoid water evaporation and incubated aerobically at 30˚C for 30 days. In order to detect the presence of precipitates during incubation, Petri dishes were observed once a day with light microscopy (20x). After the incubation period was completed, precipitates were recovered by scraping the colony from the agar surface. Subsequently, they were washed several times with distilled water to eliminate the nutritive solution, remaining agar and cellular debris and dried at 37 ˚C. Microscopic observation demonstrated that this treatment does not alter the morphology of the crystals.

pH measurements were performed at the end of the growth and carbonate formation experiments. pH-indicator paper (Merck Spezial-Indikatorpapier) was directly applied to the semi-solid surface.

X-ray diffraction analysis

The purified minerals formed in the laboratory culture experiments by the two different bacteria strains were powdered and analyzed for their mineralogy on a Bruker AXS D8 Advance Bragg-Brentano X-ray diffractometer (XRD). The samples were scanned by continuous scan at 1˚/min from 5 to 70˚ with Cu-Kα radiation. From the d_{104} of the diffraction spectra, the Mg/Ca ratio of the carbonate minerals was calculated after Lumsden (1979).

Scanning electron microscope analysis

The microbial precipitates from culture experiments and geological samples were prepared for scanning electron microscopic (SEM) observation. In order to preserve the biologic structure as well as possible, the following treatment was applied to the geological samples in the laboratory: samples were fixed with 2.5 % glutaraldehyde in 0.2 M Na-cacodylate buffer for 90 min at 4 ˚C. Subsequently, the samples were washed twice with distilled water, 30 % ethanol, dehydrated in acetone, and finally critical-point dried in liquid CO_2. Samples were analyzed by a field emission SEM equipped with an electron dispersive detector (EDS) (Leo 1530, 143 eV resolution, LEO Electron Microscopy LTD, Germany).

Methods for transmission electron microscopy (TEM), atomic force microscopy (AFM) and Raman microscopy

For these studies culture experiments using *H. meridiana* were carried out. The microbial precipitate was analyzed by TEM, AFM and Raman microscopy after 10 days of incubation, when the crystal precipitates were visible by optical microscopy. Sub-samples were prepared by scraping a small quantity of the bacteria off of *H. meridiana* culture plates with a sterile loop and transferring into a centrifuge tube containing nanopure water. After centrifugation at 3000g for 10 minutes the supernatant was drawn out and cells were again resuspended in fresh nanopure water. This washing procedure was repeated three times.

For TEM analyses, a drop of resuspended subsample was pipetted onto collodium/carbon-coated 200 mesh copper grids and air-dried for 1-2 hours. The samples were analyzed under Philips CM 12, 100KV TEM with a CCD camera model 794. Mica disks were cleaved several times to obtain thin individual disks. A drop of subsample was placed on a mica disk and was allowed to stand for 30 minutes, and allowed to dry for imaging in air.

For AFM and Raman microscopy analyses, resuspended material was pipetted onto glass cover slips. The experimental apparatus consists of an inverted confocal laser-scanning microscope (FluoView FV500, Olympus, Melville, NY) combined with a Raman spectrograph (Holospec *f*/1.8*i*, Kaiser Optical Systems, Ann Arbor, MI) and an AFM (Explorer, Veeco Instruments, Santa Barbara, CA). A more detailed description of the setup, which allows simultaneous investigation of the exactly same spot of a sample with different techniques, can be found in the literature (Vannier *et al.*, 2006). AFM imaging was performed in tapping mode using silicon tips (NSC15/Al BS, MikroMasch /

Schaefer-Tec, Kirchberg, Switzerland). For collection of Raman spectra of nanoglobules, the AFM tip was placed on the structure and a 532-nm laser beam (Ventus, Laser Quantum, Stockport, UK) was focused onto the tip apex with the help of the confocal scanning optics. In this way, precise positioning of the laser focus on nanoglobules, which were not resolved in the confocal microscope image, was possible. For both, excitation and collection of Raman scattering, a 60x / 1.4 N.A. oil immersion objective was employed.

Bulk powdered biogenic dolomite was investigated as a reference sample using an upright confocal Raman microscopy setup (NTegra spectra, NT-MDT, Zelenograd/Moscow, Russia) with 632.8-nm excitation (HeNe laser, Thorlabs, Dachau/Munich, Germany). Before collection of Raman spectra, the sample spot under investigation was bleached by laser irradiation for 1 h in order to reduce the fluorescence emission from organic contaminants. Excitation in the red spectral range reduced the fluorescence background, which hampered the detection of Raman bands using the inverted microscope setup with 532-nm excitation even after bleaching.

Raman microscopy of the EPS film

The Raman spectrum in Figure DR2 was collected as an average of three measurements with an acquisition time of 60 s each. The spectrum can be assigned to a mixture of different organic compounds. In contrast to the dolomite spectra (Fig. 1C), it contains several broad and sharp bands, most of them clearly outside the typical range of carbonate minerals between 1000 and 1200 cm^{-1} (Edwards *et al.*, 2005a).

The band at 1726 cm^{-1} can be assigned to a C=O stretching vibration in the typical range of the C=O signals of lipids (Grdadolnik *et al.*, 1998; Takai *et al.*, 1997). Raman intensity in the amide I range between 1660 and 1670 cm^{-1} (Schuster *et al.*, 2000) is very weak. The strong bands at 1600 and 1577 cm^{-1} are in the range of C=C double bond stretching vibrations, where the latter can be assigned to conjugated double bonds, e.g. in pigments (Edwards *et al.*, 2005b). In general, we expect that signals from pigments are relatively strong due to resonance Raman enhancement. The broad band at 1450 cm^{-1} is a good marker for organic material in general, because the CH_2 scissoring vibrations in this range can be detected in many organic substances, such as lipids and polysaccharides (Edwards *et al.*, 2005b; Schuster *et al.*, 2000; Takai *et al.*, 1997). Also in many different organic / biological systems, a broad signal in the range of 1250-1350 cm^{-1} can be found, which is a superposition of =C-H bending and CH_2 twisting vibrations with contributions from the amide III mode (Edwards *et al.*, 2005b; Schuster *et al.*, 2000; Takai *et al.*, 1997) and is represented in our case by the signal at 1289 cm^{-1}. The range between 1000 and 1200 cm^{-1} is characterized by C-C single bond stretching vibrations and contributions from C-N and C-O vibrations. The band at 1162 cm^{-1} is most probably the C-C single bond vibration corresponding to the 1577 cm^{-1} C=C vibration of conjugated double bond systems (Edwards *et al.*, 2005b). For the sharp bands at 1125 and 1039 cm^{-1} an assignment to both, C-C of organic material and carbonate stretching vibrations of minerals is possible. The literature reports the strongest band in the Raman spectrum of hydromagnesite at 1120 cm^{-1} (Edwards *et al.*, 2005a), the band at 1039 cm^{-1} represents probably an unknown / amorphous form of a carbonate mineral or represents C-C stretching vibrations of organic material.

We can conclude that the Raman spectrum supports the presence of an organic EPS film containing different species. The bands can be tentatively assigned to lipids, polysaccharides, and pigments with conjugated double bonds. Since strong bands in the amide I range are missing, proteins most probably play a minor role in the EPS composition. We expect to get more specific information on the organic compounds directly associated with minerals by tip-enhanced Raman spectroscopy (TERS), which provides spatial resolution in the nanometer range (Stöckle *et al.*, 2000; Schmid *et al.*, 2007).

Table DR1. Biochemical conditions of the culture media before and after mineral precipitation.

Culture	T (˚C)	[a]pH	Time (days) Growth	Begin Precipitation	Extensive Precipitation	[b]pH	d_{104} (Å)	[c]Formula for dolomite
V. marismortui	25	7.2	2	4	12	8.5	2.902	$Ca_{1.10}Mg_{0.90}(CO_3)_2$
V. marismortui	35	7.0	1	3	9	8.5	2.893	$Ca_{1.06}Mg_{0.94}(CO_3)_2$
H. meridiana	25	7.4	2	5	12	8.5	2.891	$Ca_{1.04}Mg_{0.96}(CO_3)_2$
H. meridiana	35	7.3	1	4	10	9.0	2.902	$Ca_{1.10}Mg_{0.90}(CO_3)_2$

(a) Starting pH in the medium; (b) Final pH in the medium; (c) The formulas were obtained from d_{104} peak of the diffraction spectra according to Lumsden (1979).

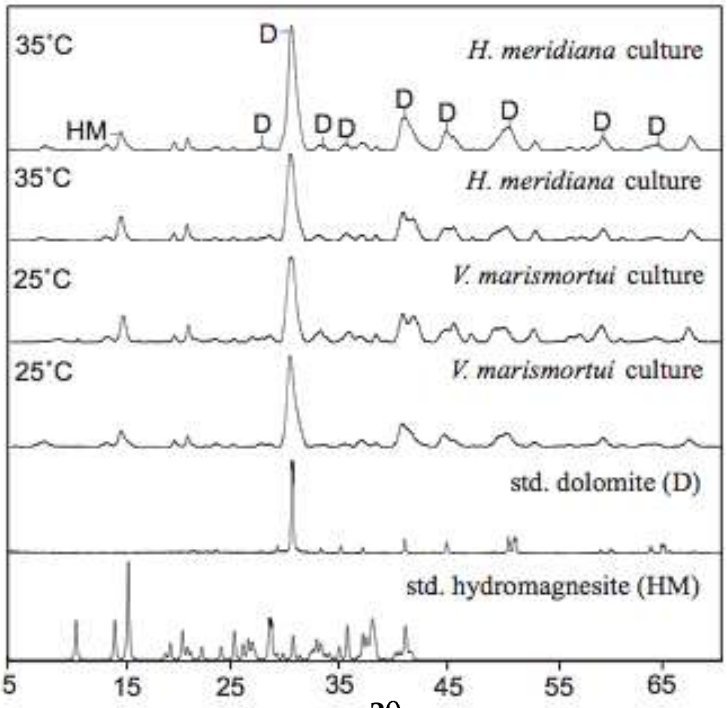

Figure DR1. X-ray diffractograms of crystals formed in cultures of *V. marismortui* and of *H. meridiana* at 25 and 35˚C. Major and secondary peaks for dolomite (D) are indicated, whereas for hydromagnesite (HM) only the major peak is indicated.

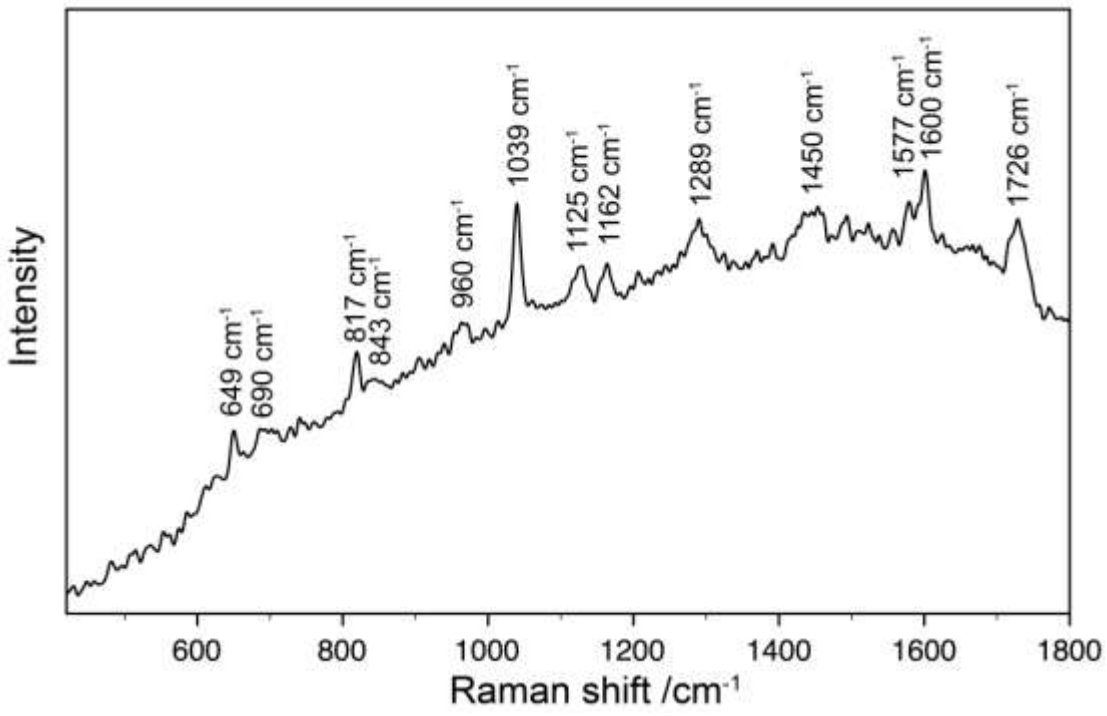

166

167 **Figure DR2: Typical Raman spectrum of the extracellular organic film (see text for**
168 **band assignments).**

169

170

171

172

173

174

175

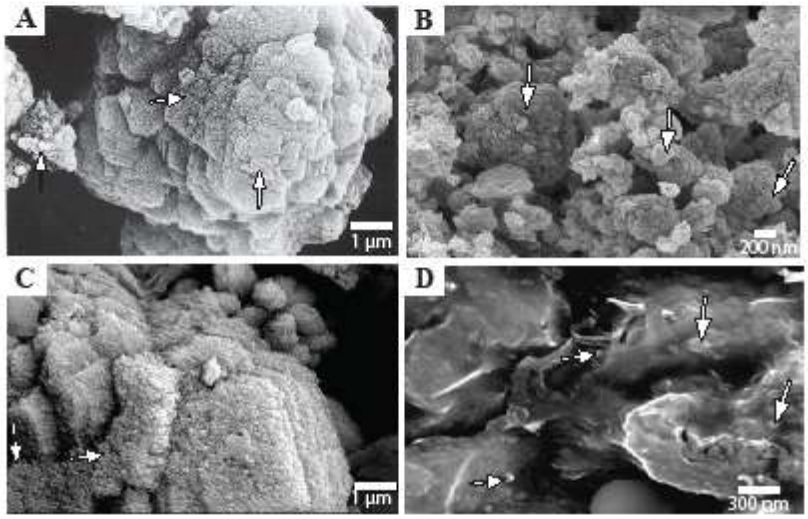

Figure DR3. SEM photomicrographs of dolomite nanocrystal aggregates showing granulated texture. Samples from modern environments: A: Lagoa Vermelha, Brazil; B: Brejo do Espinho lagoon, Brazil. C: Abu Dhabi, United Arab Emirates. D: Archean Dolomite from the Warrawoona Group with possible globules on its surface. Note that dolomite crystals are formed by aggregates of nanoglobules (indicated by arrows). These nanoglobules range from 30 to 100 nm in diameter.

References

Arahal, D.R., Marquez, M.C., Volcani, B.E., Schleifer, K.H., and Ventosa, A., 1999, *Bacillus marismortui* sp. Nov., a new moderately halophilic species from the Dead Sea: International Journal of Systematic Bacteriology, v. 49, p. 521-530.

Edwards, H.G.M., Villar, S.E.J., Jehlicka, J., and Munshi T., 2005a, FT-Raman spectroscopic study of calcium-rich and magnesium-rich carbonate minerals: Spectrochimica Acta Part A, v. 61, p. 2273-2280.

Edwards, H.G.M., Moody, C.D., Newton, E.M., Villar, S.E.J., Russell, M.J., 2005b,

193 Raman spectroscopic analysis of cyanobacterial colonization of hydromagnesite, a
194 putative martian extremophile: Icarus, v. 175, p. 372-381.
195 Grdadolnik, J., and Hadzi, D., 1998, FT infrared and Raman investigation of
196 saccharide-phosphatidylcholine interactions using novel structure probes:
197 Spectrochimica Acta Part A, v.54, p. 1989-2000.
198 James, S.R., Dobson, S.J., Franzmann, P.D., and McMeekin, T.A., 1990, *Halomonas*
199 *meridiana*, a new species of extremely halotolerant bacteria isolated from Antarctic
200 saline lakes: Systematic & Applied Microbiology, v. 13, p. 270-277.
201 Lumsden, D.N., 1979, Discrepency between thin-section and X-ray estimates of dolomite
202 in limestone: Journal of Sedimentary Petrology, v. 49, p. 429-435.
203 Oren, A., 2002, Halophilic microorganisms and their environments, in: Seckbach, J.
204 (Ed.), Cellular Origen and Life in Extreme Habitats, vol. 5. Kluwer Academic,
205 Dordrecht, The Netherlands, 600 pp.
206 Sánchez-Román, M., 2006, Calibration of Microbial and Geochemical Signals Related to
207 Dolomite Formation by Moderately Halophilic Aerobic Bacteria: Significance and
208 Implication of Dolomite in the Geologic Record, PhD Dissertation Nr. 16875, ETH-
209 Zürich, Switzerland.
210 Sánchez-Román, M., Vasconcelos, C., Warthmann, R., Rivadeneyra, M., and McKenzie,
211 J.A., XXXX, Microbial dolomite precipitation under aerobic conditions: Results
212 from Brejo do Espinho Lagoon (Brazil) and culture experiments, *in* Swart, P.K.,
213 Eberli, G.P., and McKenzie, J.A., eds, Perspectives in Sedimentary Geology: A
214 Tribute to the Career of Robert Nathan Ginsburg: International Association of

Sedimentologists Special Publication 41, *in press*.
(http://mgg.rsmas.miami.edu/rnggsa/sanchezfinal.pdf).

Schmid, T., Yeo, B.S., Zhang, W., and Zenobi, R., 2007, Use of Tip-enhanced Vibrational Spectroscopy for Analytical Applications in Chemistry, Biology, and Materials Science, in: S. Kawata and V. Shalaev (eds.) Tip Enhancement, Elsevier, Amsterdam, p. 115-156.

Schuster, K.C., Reese, I., Urlaub, E., Gapes, J.R., and Lendl, B., 2000, Multidimensional Information on the Chemical Composition of Single Bacterial Cells by Confocal Raman Microspectroscopy: Analytical Chemistry, v. 72, p. 5529-5534.

Stöckle, R.M., Suh, Y.D., Deckert, V., and Zenobi, R., 2000. Nanoscale chemical analysis by tip-enhanced Raman spectroscopy: Chemical Physics Letters, v. 318, p.131-136.

Takai, Y., Masuko, T., and Takeuchi, H., 1997, Lipid structure of cytotoxic granules in living human killer T lymphocytes studied by Raman microspectroscopy: Biochimica et Biophysica Acta, v. 1335, p. 199-208.

Vannier, C., Yeo, B.S., Melanson, J., and Zenobi, R., 2006, Multifunctional microscope for far-field and tip-enhanced Raman spectroscopy: Review of Scientific Instruments, v.77, p. 023104-1-5.